NANOSYSTEMS: PHYSICS, CHEMISTRY, MATHEMATICS, 2014, 5 (2), P. 210–216

OPTICAL INDUCTION OF 3D REFRACTIVE LATTICES IN DOUBLY DOPED $LiNbO_3$ PHOTOREFRACTIVE CRYSTAL

A. Badalyan[1], P. Mantashyan[1], V. Mekhitaryan[1], V. Nersesyan[1*] and R. Drampyan[1,2]

[1]Institute for Physical Research, National Academy of Sciences of Armenia, 0203, Ashtarak-2, Armenia

[2]Armenian – Russian (Slavonic) University, H. Emin str. 123, 0051, Yerevan, Armenia

*vars.nersesyan@gmail.com

PACS 42.70.Qs, 78.67.Pt

The optical induction of 3D rotational symmetry refractive lattices in doubly doped photorefractive and photochromic $LiNbO_3$:Fe:Cu crystal by combined interferometric-mask method was performed. The method is based on the spatial light modulation by amplitude mask in the transverse plane and the use of counter-propagating beam geometry building up a Gaussian standing wave, which defines the light intensity modulation in the axial direction with half-wavelength periodicity. Masks with rotationally symmetrical structures are used in the experiment. The created intensity pattern was imparted into the $LiNbO_3$:Fe:Cu crystal thus creating refractive lattice with the periods of 20 – 60 μm in the radial and azimuthal directions and 266 nm in the axial direction. The refractive and dispersive properties of the recorded lattices were studied.

Keywords: Photonic lattice, photorefractive and photochromic effects, lithium niobate, micro- and nano-structures.

1. Introduction

Light controlling systems, such as two- and three-dimensional (2D, 3D) photonic crystals and optically induced refractive lattices are of great interest for various applications, including guiding and trapping systems, photonic bandgap materials, all-optical devices, information storage and processing, telecommunication systems, optical computers, etc.

There are well known methods for creating the refractive structures by electronic beam, UV lithography or etching techniques which permit the formation of micro- and nano-scale permanently fixed refractive structures in the materials with high refractive index, providing pronounced photonic bandgaps. The holographic technique is based on the illumination of a photorefractive medium by spatially modulated light beam which leads to the corresponding refractive index modulation and creates refractive lattices in the medium (photonic lattices). The optical induction methods provide relatively low refractive index contrast. Nevertheless such an approach becomes particularly attractive for applications which require the ability to tune and adapt photonic lattices in real time. Photonic lattices are very promising for high capacity information storage and readout [1], for controlling and manipulating the light flow [2], and higher order rotational symmetry 3D lattices provide the appearance of isotropic and complete photonic bandgaps [3, 4]. Photorefractive crystals are one of the promising photosensitive materials for the formation of photonic lattices.

Recently, we suggested the combined interferometric–mask method (CIM) [5, 6] for formation of 3D photonic lattices. The main concept was the combination of a well known computer generated mask technique, providing the formation of 2D gratings with two-beam interference method, providing the formation of 1D gratings. Our approach is based on the spatial light modulation by amplitude mask in the transverse plane and the use of counter-propagating beam geometry building up Gaussian standing wave, which defines the light intensity modulation in the axial direction with half-wavelength periodicity. The created intensity patterns can be imparted into the photorefractive medium and create micro- and nano-scale 3D refractive index volume lattices. In fact, the formed 3D intensity pattern is an assembly of numerous mask-generated 2D periodic or quasi-periodic structures located in each anti-node of the standing wave. Thus, the CIM method allows the optical induction of 3D photonic lattices with the nanoscale 200 – 300 nm lattice periodicities along the axial direction. The method was realized in $LiNbO_3$:Fe crystal with the use of 7-fold rotational symmetry mask in [5] and 2-fold rotational symmetry mask in [6].

In this paper, we present the experimental results for the study of 3D refractive lattice formation in doubly doped lithium niobate (LN) crystals with the use of a 2-fold rotational symmetry amplitude mask. In the experiment, the LN:Fe:Cu crystal was used since doubly doped photorefractive crystals reveal also the photochromic effect, i.e. the dependence of the absorption coefficient on light intensity [7]. Photochromic properties provide the decreasing of the erasure of the lattices during readout by weaker probe beam at the recording wavelength. The photochromic properties of LN:Fe:Cu crystal allowed us to study the dispersive properties of refractive lattices by diffraction of white light from the lattices.

2. Optical induction of 3D refractive lattices

The 3D refractive lattices were optically induced by combined interferometric-mask method in a $LiNbO_3$ crystal doped by 0.05 wt% Fe and Cu (LN:Fe:Cu). The photorefractive LN:Fe:Cu crystal was illuminated through the 2-fold rotational symmetry micrometric scale mask by cw 532 nm, 100 mW laser beam in combination with back reflecting mirror (Fig. 1) over 30 – 60 min. The counter-propagating beam geometry builds up a Gaussian standing wave, which determines the half-wavelength periodic light modulation in the axial direction.

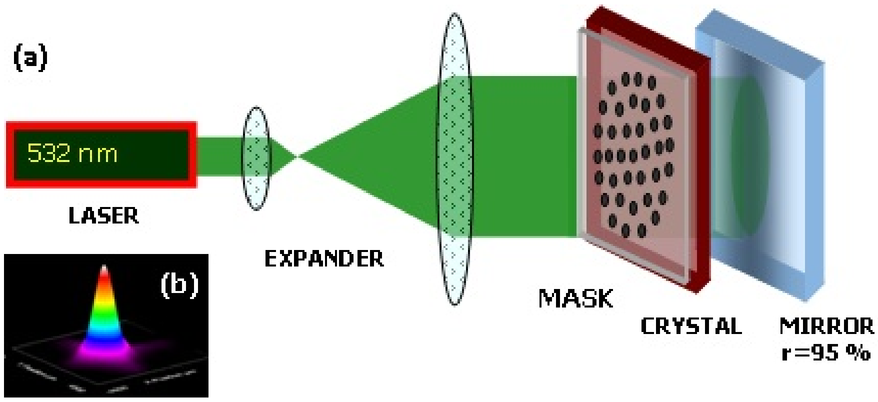

FIG. 1. (a) Experimental setup for induction of 3D lattices by CIM method. Removing the back reflecting mirror leads to the formation of 2D lattices with refractive index modulation in the transverse plane, (b) the Gaussian intensity distribution of the laser beam with the wavelength of 532 nm

Figure 2a shows the fragment of the used 2-fold rotational symmetry mask. The prepared negative mask had a distance of 20 – 60 μm between 10 μm transparent holes on the opaque disk. The mask consists of $\sim$ 10,000 holes disposed along the 100 hypothetical concentric circles. The technique of mask preparation is described in detail elsewhere [5,6]. The diffraction patterns from the mask were obtained in the far field by a red 633 nm He-Ne single mode laser beam, as well as by a light emitted diode (LED) source emitting white light as a mix of the emissions in blue (480 nm), green (570 nm) and red (640 nm) spectral ranges. The diffraction patterns are shown in Fig. 2b and c, respectively. In the case of the LED source, the emitted light after passing through the 1mm diaphragm illuminates the mask placed 150 cm from the diaphragm. The high contrast diffraction patterns from the mask confirm the high quality of the prepared masks.

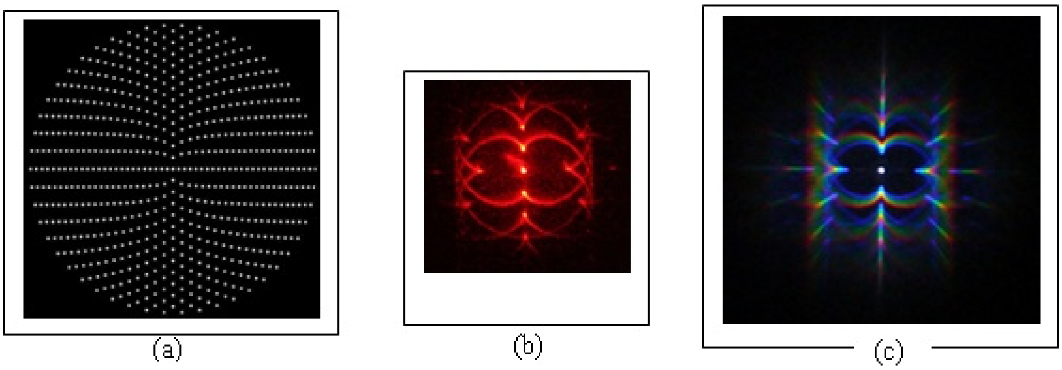

FIG. 2. (a) Fragment of 2-fold rotational symmetry mask. (b) and (c) are far field diffraction patterns from the mask obtained by red 633 nm laser beam and tricolor LED source, respectively

The formed 3D rotational symmetry photonic lattice inside the crystal represents itself a set of numerous mask-generated 2D quasi-periodic structures located in each anti-node of the standing wave and has 20 – 60 μm periods in the radial and azimuthal directions and half-wavelength 266 nm period in the axial direction (Fig. 3). The 2D lattice, modulated only in the transverse plane, can be recorded by simply removing the back reflecting mirror shown in Fig. 1.

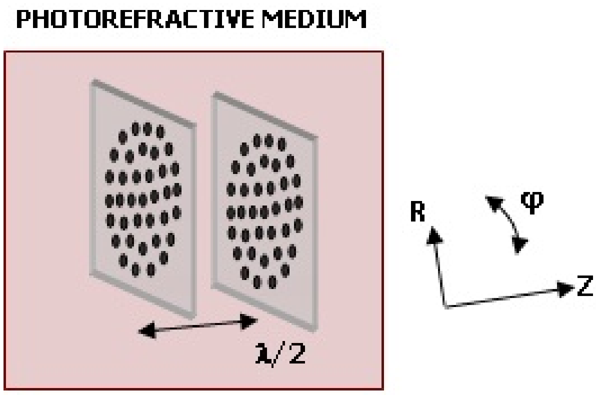

FIG. 3. Schematic of two neighboring anti-nodes of standing wave, where the mask created quasi-periodic structures are located. The scale along the direction of standing wave (Z-axis) is enlarged relative to R and φ directions

3. Optical testing of the recorded refractive lattices

The optical testing of the recorded lattices was performed by observation of the diffraction patterns from the 3D lattices in the far field using a monochromatic 633 nm probe laser beam. The results are shown in Fig. 4a. The testing beam wavelength of 633 nm was used to decrease the erasure of the recorded lattices during the readout.

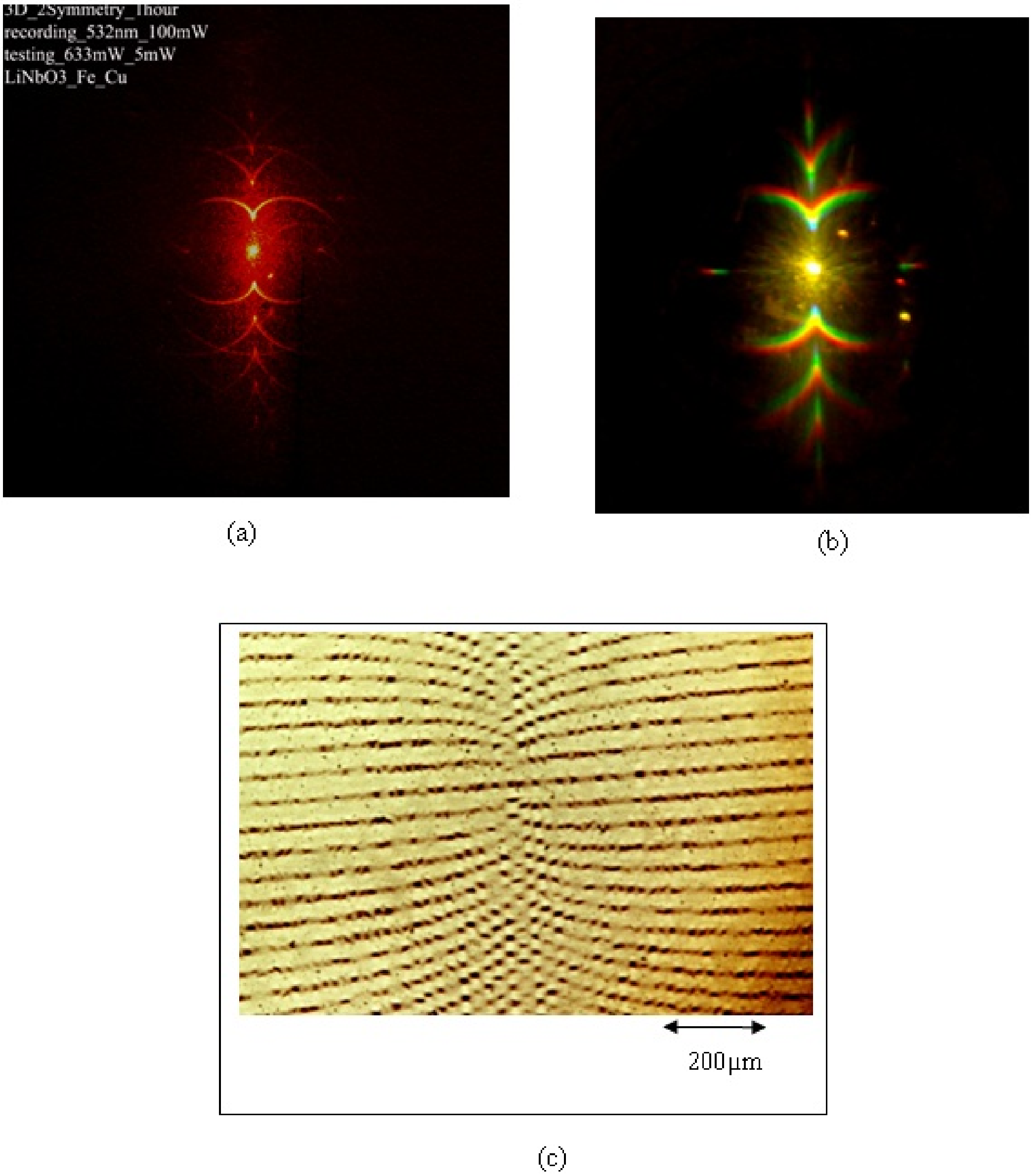

FIG. 4. (a, b) Far field diffraction patterns from recorded 3D lattice obtained by red 633 nm beam (a) and tricolor LED source (b), respectively. (c) Fragment of phase microscope images of transverse X-Y plane of 3D photonic lattices recorded inside of 2 mm thick LN:Fe:Cu crystal by 2-fold symmetry mask and 100 mW green laser beam during 1 hour

The dispersive properties of the recorded 3D volume refractive lattices have been studied by diffraction testing with the use of a tricolor LED source. The far field diffraction pattern is shown in Fig. 4b. The absence of the blue color contour in diffraction pattern is due to the strong absorption of blue light in the crystal. Fig. 4b shows that the diffraction efficiency of recorded pattern is approximately equal for visible spectral range.

The diffraction efficiency of recorded 3D lattice was measured from testing experiment with the use of an e-polarized 633 nm probe laser beam with an input power $P_{input} = 16.5$ mW.

Diffraction efficiency η was calculated as $\eta = P_{dif}/P_{input} = \{(P_{sc} - P_{bg})/P_{input}\} \times 100\%$, where the diffracted power P_{dif} is determined as a total forward scattered power P_{sc} minus background power P_{bg} transmitted through the clean part of crystal without recorded lattice, and equaled 2.3 %.

The direct observation of recorded lattices by phase microscope was also performed. Fig. 4c shows the phase microscope image of the transverse X-Y plane of 3D lattice recorded in LN:Fe:Cu crystal. The interference contrast observation was performed. The microscope allowed to strictly reveal the refractive index lattice with estimated refractive index modulation of $\delta n \sim 10^{-4} - 10^{-5}$, however, it did not allow one to perform quantitative measurements.

4. Discussion

The interest of holographic recording in doubly doped LN:Fe:Cu crystal is connected with photochromic properties of this crystal, namely the increase of absorption coefficient with the intensity of illuminating light [7, 8]. This allows the decreasing of erasure of stored lattices during readout by weaker probe beam at the recording wavelength [7].

The physical mechanism of holographic recording is connected with electro-optic effect. The illumination of photorefractive crystals by inhomogeneous light redistributes photo-charges, excited by photo-ionization, builds up internal electric field E, and so, changes the refractive index via electro-optic effect, $\delta n = 0.5 r_{33} E$, where r_{33} is electro-optic coefficient, thus allowing the induction of photonic refractive lattice structures. The electric field, induced due to spatial charge separation, is caused by the photovoltaic effect and diffusion of the photo-induced charge carriers. The photocurrent density J, along the crystalline C-axis due to the photovoltaic effect, equals $J = k_1 \alpha I$, where k_1 is Glass constant depending on the nature of absorbing centers and light wavelength, α is absorption coefficient and I is light intensity [9, 10]. The diffusion of charge carriers takes place in all directions and can be neglected for lattice spatial frequencies $K = 1/d$ having the values less than $\sim 10^5$ lines/cm, where d is the lattice period [9].

In comparison to the singly doped LN:Cu crystal, where electrons excited from Cu^{1+} are captured by Cu^{2+} centers, the doubly doped LN:Fe:Cu crystal also has Fe^{2+} center photo-excited electrons , move to the conductivity band and then are captured by both Fe^{3+} and Cu^{2+}. The capturing by Cu^{2+} forms additional Cu^{1+} centers. The increase of the ratio of Cu^{1+}/ Cu^{2+} leads to an increase in the absorption coefficient of the crystal [7, 8, 11]. The band diagram for two-center recording is shown in Fig. 5.

It is worth noting that the diffraction efficiency of 3D lattice recorded in LN:Fe:Cu crystal is lower than for the lattices recorded in LN:Fe crystal [5,6]. This is connected with lower value of the Glass constant and larger value of photoconductivity in LN:Fe:Cu crystal, while the absorption coefficients of LN:Fe and LN:Fe:Cu at 532 nm wavelength are approximately the same. The diffraction efficiency of the lattice in LN:Fe:Cu crystal can be increased by optimization of Fe and Cu concentration in the LN crystal, since conductivity depends on the dopant ions' concentrations.

The life-time of recorded lattices in the doped lithium niobate crystals in the absence of external affects, such as light and heating is up to one year [12, 13]. At room temperature, the dark storage time of recorded lattices in LN:Fe:Cu crystal, which are used in the present experiment is more than a period of one year. The recorded structures can be erased by homogeneous light, more effectively by intense UV light, thus allowing the multiple recording and readout of photonic structures in the crystal.

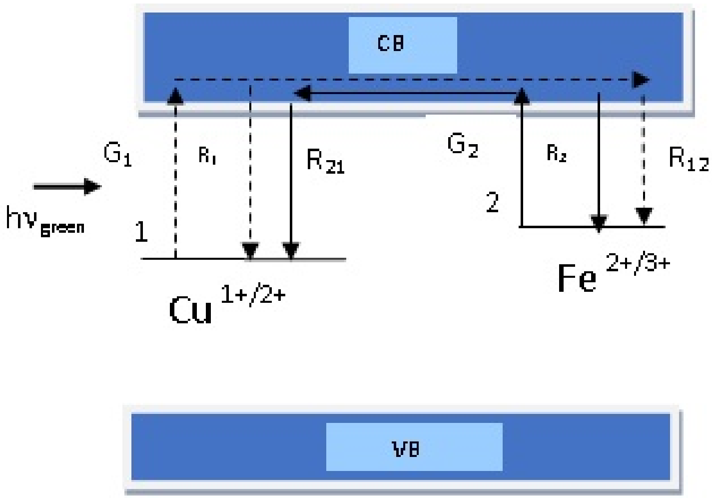

FIG. 5. Band diagram of the two-center charge transport model. CB is the conduction band, VB is the valence band. Arrows indicate excitation and recombination of electrons at Cu^{1+}/Cu^{2+} and Fe^{2+}/Fe^{3+}. G_1, G_2 are absorption cross sections, R_1, R_2 are recombination rates of Fe and Cu centers. R_{12}, R_{21} are recombination rates between Cu–Fe and Fe–Cu centers, respectively (see [8, 11])

5. Conclusion

The recording of 3D photonic lattices in photorefractive LN:Fe:Cu crystals, also revealing a photochromic effect, was realized by an interferometric-mask method. The formed 3D lattices had 20 – 60 μm periods in the radial and azimuthal directions and 266 nm period in the axial direction. The recorded lattices were tested by diffraction of 633 nm probe laser beam, as well as by white light which revealed the dispersive properties of the lattice. Direct observation of recorded lattices by phase microscope was also performed. The diffraction efficiency of recorded lattice was measured at 2.3 %.

2D and 3D periodic and quasi-periodic photonic structures in photorefractive materials are promising for many applications, including guiding and trapping systems, photonic bandgap materials, all-optical devices, high capacity information storage and processing, spatial soliton formation, telecommunication systems, optical computers etc.

Acknowledgments

This work was supported by International Science and Technology Center Grant, Project A-1517 and National Grant of State Committee of Science of Armenia, Project 1-6/HK.

References

[1] A. Adibi, K. Buse, D. Psaltis. Two-center holographic recording. *JOSA B*, **18**, P. 584–601 (2001).
[2] K. Buse, C. Denz, W. Krolikowski. Photorefractive materials, effects, and devices: control of light and matter. *Appl. Phys. B*, **95** (3), P. 389–390 (2009).
[3] M.E. Zorob, M.D.B. Charlton, et al. Complete photonic bandgaps in 12-fold symmetric quasicrystals. *Nature*, **404**, P. 740 (2002).
[4] W. Man, M. Megens, P.G. Steinhardt, P.M. Chaikin. Experimental measurement of the photonic properties of icosahedral quasicrystals. *Nature*, **436**, P. 993 (2005).
[5] A. Badalyan, R. Hovsepyan, et al. Combined interferometric-mask method for creation of micro- and submicrometric scale 3D structures in photorefractive materials. Proceedings of SPIE, International Conference on Laser Physics 2010, **7998**, P. 7998OH-1–10 (2011).

[6] A. Badalyan, T. Gevorgyan, et al. Engineering of 2D and 3D holographic gratings in photorefractive media. Proceedings of SPIE, Photonics and Micro- and Nano-structured Materials 2011, **8414**, P. 8414 05-1–11 (2012).

[7] P. Mantashyan. Photochromic effect and holographic recording in doubly doped $LiNbO_3$ crystals. Proceedings of SPIE, International Conference on Laser Physics 2010, **7998**, P. 7998OJ-1–9 (2011).

[8] G.T. Avanesyan, E.S. Vartanyan, et al. Mechanisms of photochromic and photorefractive effects in doubly doped lithium niobate crystals. *Physica Status Solidi A*, **126** (1), P. 245–252 (1991).

[9] A.M. Glass, D. von der Linde, T.J. Negran. High-voltage bulk photovoltaic effect and the photorefractive process in $LiNbO_3$. *Appl. Phys. Lett.*, **25**, P. 233–235 (1974).

[10] F.S. Chen. Optically induced change of refractive indices in lithium niobate and lithium tantalate. *J. Appl. Phys.*, **40**, P. 3389 (1969).

[11] K. Buse. Light-induced charge transport processes in photorefractive crystals. *Appl. Phys. B*, **64** (3), P. 273–291 (1997).

[12] Y. Yang, I. Nee, K. Buse, D. Psaltis. Ionic and electronic dark decay of holograms in $LiNbO_3$:Fe crystals. *Appl. Phys. Lett.*, **78**, P. 4076 (2011).

[13] I. Nee, M. Muller, K. Buse, E. Kratzig. Role of iron in lithium-niobate crystals for the dark-storage time of holograms. *J. Appl. Phys.*, **88**, P. 4282 (2000).